

# Mathematical Simulation and Design of a Rectangular Cavity of Microwave Pretreatment Equipment Used for Wood Modification

Xi Li,<sup>a</sup> Jianxiong Zhang,<sup>a</sup> Chunrong Liao,<sup>a</sup> Hongbin Chen,<sup>a</sup> Yongfeng Luo,<sup>a,\*</sup> and Xianjun Li<sup>b,\*</sup>

Wood pretreated by high-intensity microwaves was theoretically studied based on the Maxwell electromagnetic field equations and the heat and mass transfer mechanism of wood. The effects of feeding modes on the temperature field uniformity and energy efficiency were studied using the finite element method, and optimized parameters of the rectangular microwave resonant cavity were achieved. The results show that the feeding modes had a great effect on the temperature field uniformity of the wood and the energy efficiency. Compared to the side single-port, the upper single-port, and the upper-under port feeding modes, the two-side ports feeding mode was the best for temperature field uniformity and energy efficiency.

*Keywords:* Wood; Microwave pretreatment; Rectangular resonant cavity; Temperature distribution; Energy efficiency

*Contact information:* a: College of Science, Central South University of Forestry and Technology, Changsha, Hunan 410004, China; b: Material Science and Engineering School, Central South University of Forestry and Technology, Changsha, Hunan 410004, China;

\* Corresponding authors: yongfengluo@csu.edu.cn (Y.F. Luo) and lxjmu@163.com (X. J. Li)

## INTRODUCTION

Microwave-induced pyrolysis of biomass for biofuels production is a widely studied topic (Wang *et al.* 2009; Balasubramanian *et al.* 2011; Wu *et al.* 2012; Yin 2012; Ren *et al.* 2013; Bu *et al.* 2014). Alternatively, microwaves can be used to treat wood in an effort to improve wood properties. High-intensity microwave pretreatment for wood drying originated from wood modification technique in Australia at the end of the last century (Turner *et al.* 1998; Oloyede and Groombridge 2000). The water in the wood absorbed energy from the transient electromagnetic waves and was transformed into steam. The impetus of steam expansion destroyed the wood micro-structure, forming new channels for fluid flow, which facilitated the wood drying process, increased the efficiency, and puffed the wood.

Research in Australia showed that after high-intensity microwave pretreatment, the density of the wood was reduced, the permeability of the wood was increased 14-fold, the preservative penetration increased 10 to 14 times, and the elasticity modulus decreased 12 to 17% (Przewloka *et al.* 2007; Torgovnikov and Vinden 2009; 2010). As a result, a novel wood composite material was prepared by puffed wood, which has high strength, large surface hardness, high water permeability, low density, and good sound insulation. The study by Antti and Perre (1999) shows that the drying proceeds unevenly in the wood specimens, and concludes that the dimensions of the applicator and wood are very

important. To predict the evolution of the variables relating to heat and mass transfer, a dynamic model was built (Carvalho *et al.* 2003).

Mathematical modelling strategies offer a cost-efficient way to optimize existing applicator design specifications (Perré and Turner 1999). In recent years, microwave pretreatment of wood has been studied by Chinese scholars at the Chinese Academy of Forestry, Northeast Forestry University, and Central South University of Forestry and Technology, and preliminary research results have been obtained (Wang *et al.* 2002; Li *et al.* 2005; Jiang *et al.* 2006; Zhou *et al.* 2009; Li *et al.* 2012). However, the existing research has some shortcomings. The most serious problem is non-uniformity of the wood microwave modification, whereby the influence of the microwave source and feed direction cannot be ignored. Uniformity of microwave-modified wood can be achieved through focused development of the microwave cavity with uniform distribution of the electromagnetic field and related microwave pretreatment devices. Thus, an electromagnetic field distribution model and heat-mass transfer model were designed to optimize the high-intensity microwave wood pretreatment process. Mathematical simulation was used to study the temperature distribution uniformity and energy efficiency influenced by microwave feeding modes.

In this manuscript, we studied the theoretical wood pretreatment by high-intensity microwaves with the Maxwell electromagnetic field equations and the heat and mass transfer mechanism of wood. The best mode for temperature field uniformity and energy efficiency was obtained.

## EXPERIMENTAL

### Methods

The distribution of the electromagnetic wave in a rectangle waveguide resonant cavity and wood temperature under different feeding modes was studied by creating the theoretical simulation of high-intensity microwave treatment. To simplify the theoretical calculations, the following assumptions were made: (1) before heating, the temperature and moisture were distributed evenly in the wood; (2) during heating, the volume of wood remained constant; (3) the wood remained static in the cavity; (4) the heat exchange between the wood surface and the air satisfied the boundary conditions of convection and heat transfer; and (5) wood is an isotropic material, such that the dielectric properties of wood are same in each direction.

The microwave electromagnetic field and temperature distribution of wood were calculated by finite element analysis. The microwave frequency was 915 MHz, and the length, width, and height of the rectangular resonator cavity were 0.495, 0.248, and 0.080 m, respectively. The total input power of the microwave excitation sources was set at 20 kW, and the power was equally allocated to each excitation source with the same phase. The feeding port of the waveguide was a standard waveguide (model number BJ9; length of 0.248 m and width of 0.124 m), and the incident angle from waveguide to rectangular cavity was 45°. The initial moisture content of wood was 60%; length, width, and height of the wood were 0.740, 0.200, and 0.060 m, respectively; and the relative dielectric constant and dielectric loss factor were 7.40 and 1.42, respectively. The initial temperature and density were 25 °C and 570 kg/m<sup>3</sup>, respectively. Thermal conductivity  $\lambda$  (W/m °C) and specific heat  $C$  (J/kg °C) were determined as follows:

$$\lambda = 0.23[1 - 0.72 \times (25 - T) / 100] \quad (1)$$

$$C = 2650 \times (1 + T / 100)^{0.2} \quad (2)$$

## Theory

### *Distribution of the electromagnetic wave and microwave energy*

According to Maxwell's equations (Yee 1966), the electromagnetic field satisfies Eqs. 3 through 6 during the microwave heating of wood:

$$\nabla \times \vec{E} = -\frac{\partial \vec{B}}{\partial t} \quad (3)$$

$$\nabla \times \vec{H} = \vec{J} + \frac{\partial \vec{D}}{\partial t} \quad (4)$$

$$\nabla \cdot \vec{B} = 0 \quad (5)$$

$$\nabla \cdot \vec{D} = \rho_c \quad (6)$$

where  $\vec{E}$  is the electric field intensity,  $\vec{H}$  the magnetic field intensity,  $\vec{B}$  the magnetic induction intensity,  $\vec{D}$  the electric displacement,  $\vec{J}$  the current density,  $\rho_c$  the free charge density (wherein,  $\vec{J} = \sigma \vec{E}$ ,  $\vec{D} = \varepsilon \vec{E}$ ,  $\vec{B} = \mu \vec{H}$ ),  $\sigma$  the conductivity,  $\varepsilon$  the dielectric constant, and  $\mu$  the magnetic permeability. According to Eqs. 3 through 6, the distribution of the electromagnetic field inside the wood can be calculated (Ayappa 1997).

In this study, the microwave excitation source consisted of time-harmonic electromagnetic fields  $\vec{E}_{10}$ , where  $\vec{E} = \vec{E}(\vec{r})e^{-i\omega t}$ ,  $\vec{H} = \vec{H}(\vec{r})e^{-i\omega t}$ ,  $\vec{r} = x\vec{i} + y\vec{j} + z\vec{k}$ ,  $\vec{B}$  and  $\vec{D}$  can be expressed as a function  $\vec{E}$  (Eq. 7) and  $\vec{H}$  (Eq. 8):

$$\nabla \times \vec{E}(\vec{r}) = i\omega\mu\vec{H}(\vec{r}) \quad (7)$$

$$\nabla \times \vec{H}(\vec{r}) = (\sigma - i\omega\varepsilon)\vec{E}(\vec{r}) = -i\omega\varepsilon^*\vec{E}(\vec{r}) \quad (8)$$

where  $\varepsilon^*$  is the complex permittivity and can be expressed as  $\varepsilon^* = \varepsilon' + i\varepsilon''$ . Equation 9 can be obtained from Eqs. 7 and 8 (Ayappa 1997):

$$\nabla \cdot \left( \vec{E} \cdot \frac{\nabla \varepsilon^*}{\varepsilon^*} \right) + \nabla^2 \vec{E} + k^2 \vec{E} = 0 \quad (9)$$

By solving Eq. 9, the electric field distribution in wood can be obtained. In this study, it was assumed that the wood dielectric was a constant value along the direction of the electric field; the first term of Eq. 9 was zero. Therefore Eq. 9 can be simplified as follows,

$$\nabla^2 \vec{E} + k^2 \vec{E} = 0 \quad (10)$$

where  $k$  depends on the dielectric properties of wood, and its expression is as follows,

$$k = \alpha + i\beta \quad (11)$$

$$\alpha = \frac{2\pi f}{c} \sqrt{\frac{\varepsilon'(\sqrt{1 + \tan^2 \delta} + 1)}{2}} \quad (12)$$

$$\beta = \frac{2\pi f}{c} \sqrt{\frac{\varepsilon'(\sqrt{1 + \tan^2 \delta} - 1)}{2}} \quad (13)$$

where  $f$  is the frequency of the microwave radiation,  $\tan \delta$  is the wood loss tangent, and its value can be calculated from Eq. 14:

$$\tan \delta = \frac{\varepsilon''}{\varepsilon'} \quad (14)$$

To calculate the electric field distribution in wood, the solutions to Eq. 10 are obtained by the following boundary conditions:

$$n \times [\vec{E}_1(\vec{r}) - \vec{E}_2(\vec{r})] = 0 \quad (15)$$

$$n \times [\vec{H}_1(\vec{r}) - \vec{H}_2(\vec{r})] = 0 \quad (16)$$

where the subscript 1 indicates air and the subscript 2 indicates wood. Equation 16 can also be expressed as a function of electric field intensity through the following expression:

$$\frac{\partial \vec{E}(\vec{r})}{\partial r} = i\mu_0 \omega \vec{H}(\vec{r}) \quad (17)$$

The analytical solution of Eq. 10 is as follows,

$$E = A_1 e^{ikr} + B_1 e^{-ikr} \quad (18)$$

where  $A_1$  and  $B_1$  depend on the boundary conditions Eqs. 15 and 16. The electric field in wood can be used to calculate the electromagnetic field energy density using the Poynting Theorem,

$$Q = \frac{1}{2} \omega \varepsilon_0 \varepsilon'' \vec{E} \cdot \vec{E}^* \quad (19)$$

where  $\varepsilon_0$  is the permittivity of vacuum and  $\vec{E}^*$  is the complex conjugate of the electric field.

#### Heat transfer model

In the microwave pretreatment process, the micro-heat balance of wood is described by Eq. 10 (Ayappa 1997),

$$\rho C_p \frac{\partial T}{\partial t} = \nabla \cdot (k_T \nabla T) + Q \quad (20)$$

where  $\rho$ ,  $C_p$ , and  $k_T$  are the density, specific heat, and thermal conductivity of wood respectively, and  $Q$  is the electromagnetic energy density in the wood.

The boundary conditions of Eq. 20 are as follows (Campañone *et al.* 2012):

$$t = 0, \quad T = T_{ini}, \quad 0 \leq x \leq L \quad (21)$$

$$t > 0, \quad -k_T \frac{\partial T}{\partial r} = h(T - T_a) + L_{vap} k'_m (C_{w,s} - C_{equi}), \quad x=0 \text{ and } x=L \quad (22)$$

where  $x = 0$  indicates the wood surface,  $L$  is the width of the wood,  $h$  heat transfer coefficient of the inner wood,  $T_a$  and  $T_{ini}$  air and wood initial temperature respectively,  $L_{vap}$  heat of vaporization of the water,  $k'_m$  mass transfer coefficient,  $C_{w,s}$  moisture content of the wood, and  $C_{equi}$  the equilibrium moisture content of the air.

### Mass transfer model

To calculate the water concentration profile, the microscopic mass balance can be described using the following equation (Marra *et al.* 2010),

$$\frac{\partial C_w}{\partial t} = \nabla(D_w \nabla C_w) \quad (23)$$

where  $D_w$  is the effective diffusivity coefficient of the wood.

The boundary conditions of Eq. 23 are provided in (Eqs. 24 and 25):

$$t = 0, \quad C_w = C_{w,ini}, \quad 0 \leq x \leq L \quad (24)$$

$$t > 0, \quad -D_w \frac{\partial C}{\partial x} = k'_m (C_{w,s} - C_{equi}) \quad x=0 \text{ and } x=L \quad (25)$$

where  $C_{w,ini}$  is the wood initial moisture content.

## RESULTS AND DISCUSSION

### Effect of Feeding Mode on Electric Field Distribution

The electric field distribution of the resonant cavity was obtained by computational simulation. To verify the simulation, it was necessary to analyze the electric field distribution. The numerical size of the electric field in Figs. 1 and 2 was the square root of the squared electric field components in  $x$ ,  $y$ , and  $z$ -axis directions. The numerical size can represent electric field intensity of each point. Figure 1 shows that the electric field was strongest near the feed entry port in all feeding modes, whereas its intensity weakened rapidly along the feed direction. The decay rate of the electric field component in the  $x$ -direction of side feeding mode (Figs. 1a and 1c) was faster than that in the upper-under feeding mode (Figs. 1b and 1d). The width of the feeding port and resonant cavity was the same, which allowed for easy propagation of the microwave. In the side feeding mode, most of the energy was focused on the vicinity of the entry port. In the side feeding mode, an intense electric field was formed between the wood and the upper or under wall of the

cavity. The dielectric constant of air was far less than that of wood, and the electric field attenuation was very small in the air. The electric field intensity shows alternative strong and weak distributions because incident and reflected waves interfered in the one side port feeding mode and two incident waves exhibited interference in the two-side ports feeding mode. In the case of the upper-under feeding mode, the electric field intensity in the wood was lower than that in the air (Fig. 2). Figures 2a and 2c indicate that the electric field intensity in the wood did not linearly decrease along the incidence direction, but was distributed in a cosine function. The microwave can penetrate into the wood to a certain depth. Figures 2b and 2d indicate that the electric field intensity in the center of the wood along the  $x$ -direction was relatively lower than that of the two-side feeding mode, the width of the wood was a slightly lower than that of the cavity, and the microwave propagated to bilateral gaps between the wood and the wall of cavity. In the side feeding mode, the electric field intensity in the center of wood was larger than that in the upper-under feeding mode (Fig. 2).

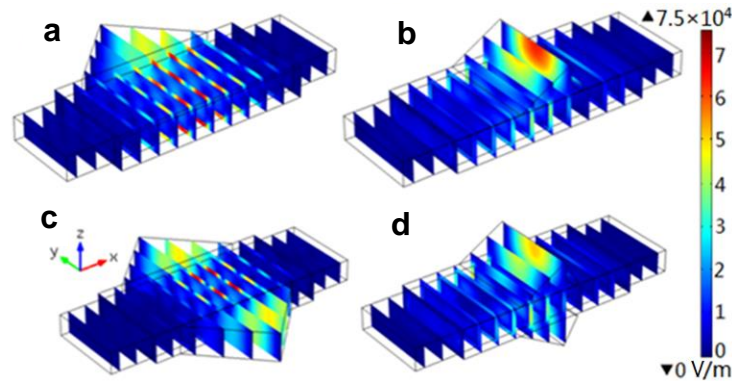


**Fig. 1.** The electric field intensity distribution in wood heated by microwave with different radiation modes: (a) side single-port feeding mode, (b) upper single-port feeding mode, (c) two-side ports feeding mode, and (d) upper and under ports feeding mode

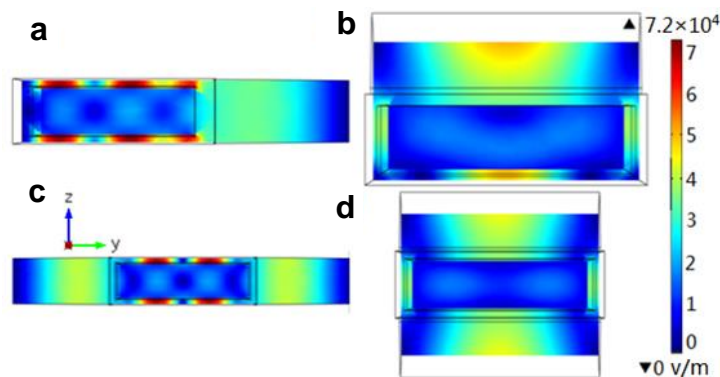


**Fig. 2.** X-direction center section of electric field distribution in wood heated by microwave with different radiation methods: (a) side single-port feeding mode, (b) upper single-port feeding mode, (c) two-side ports feeding mode, and (d) upper and under ports feeding mode

According to the Poynting Theorem, the energy absorbed is proportional to the square of the electric field intensity in the materials. Thus, the energy efficiency of the side feeding mode was higher than that of the upper-under feeding modes. Figure 2c indicates that the electric field intensity in the wood was distributed uniformly and that the two

incident waves were symmetrical. Importantly, the electromagnetic frequency matches the shape of the resonant cavity. Figure 2c also shows that the electric field intensity was not very strong near the feeding port, whereas most of the electromagnetic waves propagated along the  $x$ -direction in the gaps between the wood and the wall of the cavity.

### Effect of Feeding Mode on Temperature Distribution and Energy Efficiency

The spatial temperature distribution and energy efficiency of each feeding mode were studied (Fig. 3). The highest temperature region of the wood occurred at the microwave entrance. For the side feeding mode, the temperature distribution in the upper and lower sides of the wood displayed a symmetrical form in the  $z$ -direction; for upper and lower feeding mode, the temperature distribution was symmetrical along the central section in the  $y$ -direction. Along the  $x$ -direction, the temperature distribution varied greatly in different sections.

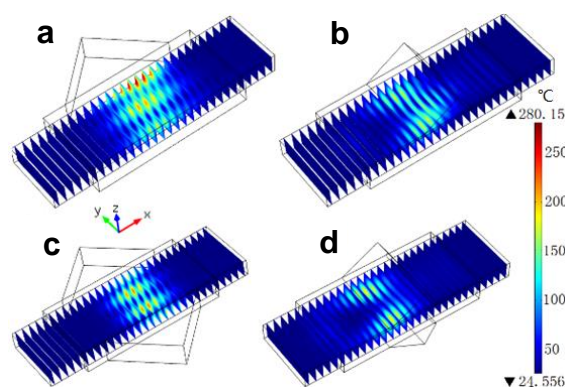


**Fig. 3.** Temperature distribution within wood heated by microwave with different radiation methods: (a) side single-port feeding mode, (b) upper single-port feeding mode, (c) two-side ports feeding mode, and (d) upper and under ports feeding mode

In the progress of microwave pretreatment, the wood would move along the  $x$ -direction, so the uniformity of temperature distribution greatly depends on the highest temperature section. Therefore, to study the uniformity of temperature distribution, the temperature profile of the central cross section near the microwave feeding port was separately extracted (Fig. 4). For the side single-port feeding mode, the temperature distribution was asymmetrical in the cross-section of wood (Fig. 4a). The high temperature region was seen near the entrance of microwave feed, and high and low temperature zones appeared alternately. A nonuniform temperature distribution is a disadvantage for high intensity microwave wood modification. Figure 4b shows the upper single-port feeding mode, where the temperature distribution in the cross section of wood along  $y$ -axis was symmetric, but was nonuniform. In the two-side ports feeding mode (Fig. 4c), the temperature distribution along the  $y$ - and  $z$ -axes was symmetrical and uniform on the cross section. For the upper-under feeding mode (Fig. 4d), the temperature distribution along the  $y$ -axes and  $z$ -axes was symmetrical; two high temperature regions were symmetrical on the cross section, but the surrounding temperature was low, and the temperature distribution was nonuniform. Microwave attenuation and microwave interference are the reasons for this. Along the direction of microwave transmission, the intensity of the microwave field will gradually decrease as interference occurs. Different feeding modes gives rise to different attenuation and interference, which have a great influence on the temperature distribution.

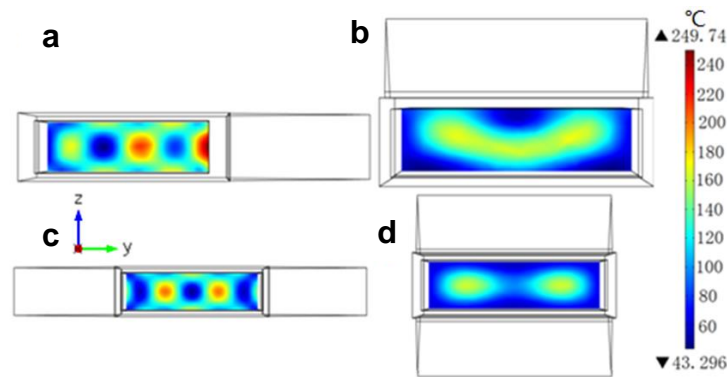


**Fig. 4.** Midsection temperature distribution within wood heated by microwave with different radiation methods: (a) side single-port feeding mode, (b) upper single-port feeding mode, (c) two-side ports feeding mode, and (d) upper and under ports feeding mode

To study the uniformity of the temperature distribution on the cross section of the wood, the temperature variation coefficient of the cross section was analyzed. It can be seen from Fig. 5 that when the wood was heated under two-side ports feeding mode, the temperature variation coefficient was the smallest thus the temperature distribution over the cross section is the most uniform. The upper single-port feeding mode was the worst among the four feeding modes.

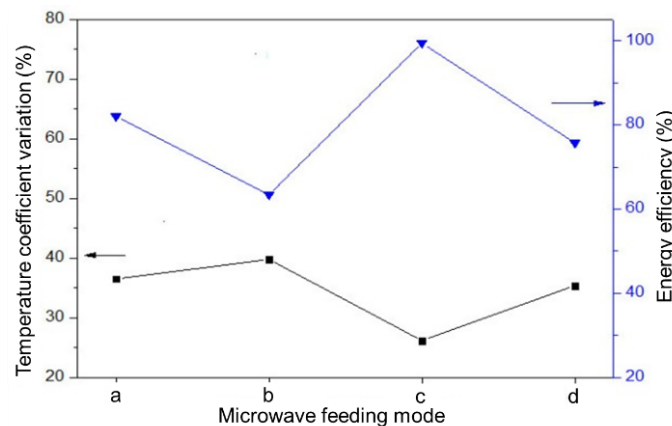


**Fig. 5.** Effect of microwave radiation methods on the temperature coefficient variation and energy efficiency. The symbols (a, b, c, and d) represent side single-port mode, upper single-port mode, two side ports mode, and upper and under ports feeding mode, respectively

To study the effect of feeding mode on energy efficiency, the energy efficiency of each feeding mode was studied. The energy efficiency of the two-side ports feeding mode was the highest (Fig. 5) because two incident waves crossed at an angle of  $90^\circ$ , which less easily led to microwave interference. The energy efficiency of the upper single-port feeding mode was the lowest, since substantial microwave interference occurred in the resonant cavity. This interference generated a standing wave, and thus a larger portion of the microwave energy was lost.

In the case of two-port feeding, the overall temperature remained at an moderate level while the maximum temperature of the central section was about  $200^\circ\text{C}$ . It was lower

than the maximum value of 240 °C, which was reached under the side single-port feeding mode. The lowest temperature reached under two-port feeding mode was 80 °C, which was higher than the upper and under feeding ports (remained at 60 °C). Energy efficiency of the two side-port feeding mode was 99.4%, which was more than 17% higher compared to the other feeding modes. Considering uniformity of temperature distribution and energy efficiency of varying feeding modes, the side two-port feeding mode is judged to be the optimal option for wood microwave treatment.

## CONCLUSIONS

1. Resonant cavities under different feeding modes were analyzed. Effect of the geometry of resonant cavity on the temperature distribution was studied, and optimized parameters of resonant cavity were obtained. The parameters were then used for the design of wood microwave pre-treatment resonant cavity.
2. Temperature field uniformity within wood and energy efficiency were affected by the feeding mode.
3. Compared with three other feeding modes, the two-side ports feeding mode showed better temperature field uniformity and higher energy efficiency.

## ACKNOWLEDGMENTS

The authors are grateful for the support of the R&D Special Fund for National Forestry Public Welfare Industry (Grant no. 201204708), the National Natural Science Foundation of China (No. 31370564), the New Century Training Program Foundation for the Talents by the Ministry of Education of China (No. NCET-11-0979), and the Graduate Student Innovation Fund of Central South University of Forestry and Technology (No. CX2014B20).

## REFERENCES CITED

- Antti, A., and Perre, P. (1999). "A microwave applicator for on line wood drying: Temperature and moisture distribution in wood," *Wood Science and Technology* 33(2), 123-138. DOI: 10.1007/s002260050104
- Ayappa, K. (1997). "Modelling transport processes during microwave heating: A review," *Reviews in Chemical Engineering* 13(2), 1-67. DOI: 10.1515/REVCE.1997.13.2.1
- Balasubramanian, S., Allen, J. D., Kanitkar, A., and Boldor, D. (2011). "Oil extraction from *Scenedesmus obliquus* using a continuous microwave system-design, optimization, and quality characterization," *Bioresour Technol* 102(3), 3396-3403. DOI: 10.1016/j.biortech.2010.09.119
- Bu, Q., Lei, H., Wang, L., Wei, Y., Zhu, L., Zhang, X., Liu, Y., Yadavalli, G., and Tang, J. (2014). "Bio-based phenols and fuel production from catalytic microwave pyrolysis

- of lignin by activated carbons,” *Bioresource Technology* 162, 142-147. DOI: 10.1016/j.biortech.2014.03.103
- Campañone, L. A., Paola, C. A., and Mascheroni, R. H. (2012). “Modeling and simulation of microwave heating of foods under different process schedules,” *Food and Bioprocess Technology* 5(2), 738-749. DOI: 10.1007/s11947-010-0378-5
- Carvalho, L., Costa, M., and Costa, C. (2003). “A global model for the hot-pressing of MDF,” *Wood Science and Technology* 37(3-4), 241-258. DOI: 10.1007/s00226-003-0170-z
- Jiang, T., Zhou, Z., and Wang, Q. (2006). “Effects of intensive microwave irradiation on the permeability of larch wood,” *Scientia Silvae Sinicae* 42(11), 87-92 (in Chinese).
- Li, X., Sun, W., Zhou, T., and Lv, J. (2012). “Mathematical modeling of temperature profiles in wood during microwave heating,” *Scientia Silvae Sinicae* 48(3), 117-121 (in Chinese).
- Li, X., Zhang, B., Li, W., and Li, Y. (2005). “Research on the effect of microwave pretreatment on moisture diffusion coefficient of wood,” *Wood Science and Technology* 39(7), 521-528. DOI: 10.1007/s00226-005-0007-z
- Marra, F., De Bonis, M. V., and Ruocco, G. (2010). “Combined microwaves and convection heating: A conjugate approach,” *Journal of Food Engineering* 97(1), 31-39. DOI: 10.1016/j.jfoodeng.2009.09.012
- Oloyede, A., and Groombridge, P. (2000). “The influence of microwave heating on the mechanical properties of wood,” *Journal of Materials Processing Technology* 100(1), 67-73. DOI: 10.1016/S0924-0136(99)00454-9
- Perré, P., and Turner, I. (1999). “The use of numerical simulation as a cognitive tool for studying the microwave drying of softwood in an over-sized waveguide,” *Wood Science and Technology* 33(6), 445-464. DOI: 10.1007/s002260050129
- Przewloka, S. R., Hann, J. A., and Vinden, P. (2007). “Assessment of commercial low viscosity resins as binders in the wood composite material Vintorg,” *Holz als Roh- und Werkstoff* 65(3), 209-214. DOI: 10.1007/s00107-006-0153-5
- Ren, S., Lei, H., Wang, L., Bu, Q., Chen, S., Wu, J., Julson, J., and Ruan, R. (2013). “The effects of torrefaction on compositions of bio-oil and syngas from biomass pyrolysis by microwave heating,” *Bioresource Technology* 135, 659-664. DOI: 10.1016/j.biortech.2012.06.091
- Torgovnikov, G., and Vinden, P. (2009). “High-intensity microwave wood modification for increasing permeability,” *Forest Products Journal* 59(4), 84-92.
- Torgovnikov, G., and Vinden, P. (2010). “Microwave wood modification technology and its applications,” *Forest Products Journal* 60(2), 173-182.
- Turner, I., Puiggali, J., and Jomaa, W. (1998). “A numerical investigation of combined microwave and convective drying of a hygroscopic porous material: A study based on pine wood,” *Chemical Engineering Research and Design* 76(2), 193-209. DOI: 10.1205/026387698524622
- Wang, X.-H., Chen, H.-P., Ding, X.-J., Yang, H.-P., Zhang, S.-H., and Shen, Y.-Q. (2009). “Properties of gas and char from microwave pyrolysis of pine sawdust,” *BioResources* 4(3), 946-959. DOI: 10.15376/biores.4.3.946-959
- Wang, X., Xue, Z., Shi, L., and Zhang, W. (2002, 16(6)). “Preliminary study on microwave modified wood,” *China Wood Industry* 16(6), 16-19.
- Wu, Y., Zhang, C., Liu, Y., Fu, Z., Dai, B., and Yin, D. (2012). “Biomass char sulfonic acids (BC-SO<sub>3</sub>H)-catalyzed hydrolysis of bamboo under microwave irradiation,” *BioResources* 7(4), 5950-5959. DOI: 10.15376/biores.7.4.5950-5959

- Yee, K. S. (1966). "Numerical solution of initial boundary value problems involving Maxwell's equations in isotropic media," *IEEE Transactions on Antennas and Propagation* 14(3), 302-307. DOI: 10.1109/TAP.1966.1138693
- Yin, C. (2012). "Microwave-assisted pyrolysis of biomass for liquid biofuels production," *Bioresource Technology* 120, 273-284. DOI: 10.1016/j.biortech.2012.06.016
- Zhou, Y.-D., Fu, F., Li, X.-J., Jiang, X.-M., and Chen, Z.-l. (2009). "Effects of microwave treatment on residue growth stress and microstructure of *Eucalyptus urophylla*," *Journal of Beijing Forestry University* 31(2), 146-150 (in Chinese).

Article submitted: August 13, 2014; Peer review completed: October 16, 2014; Revised version received and accepted: November 18, 2014; Published: November 25, 2014.